Large area deep ultraviolet light of $Al_{0.47}Ga_{0.53}N/Al_{0.56}Ga_{0.44}N$ multi quantum well with carbon nanotube electron beam pumping

Sung Tae Yoo, (iD) Byeongchan So, Hye In Lee, et al.

View Online   Export Citation   CrossMark

ARTICLES YOU MAY BE INTERESTED IN

Deep-ultraviolet light source with a carbon nanotube cold-cathode electron beam
Journal of Vacuum Science & Technology B **36**, 02C103 (2018); https://doi.org/10.1116/1.5004621

Dominance of radiative recombination from electron-beam-pumped deep-UV AlGaN multi-quantum-well heterostructures
Applied Physics Letters **109**, 181105 (2016); https://doi.org/10.1063/1.4967220

150 mW deep-ultraviolet light-emitting diodes with large-area AlN nanophotonic light-extraction structure emitting at 265 nm
Applied Physics Letters **110**, 141106 (2017); https://doi.org/10.1063/1.4978855

Call For Papers!

AIP Advances

SPECIAL TOPIC: Advances in Low Dimensional and 2D Materials

Large area deep ultraviolet light of $Al_{0.47}Ga_{0.53}N$/$Al_{0.56}Ga_{0.44}N$ multi quantum well with carbon nanotube electron beam pumping

Sung Tae Yoo,[1,a)] Byeongchan So,[2,a)] Hye In Lee,[1] Okhyun Nam,[2,b)] and Kyu Chang Park[1,b)]

AFFILIATIONS

[1] Department of Information Display, Kyung Hee University, Dongdaemun-gu, Seoul 02447, South Korea
[2] Convergence Center for Advanced Nano Semiconductor (CANS), Department of Nano-optical Engineering, Korea Polytechnic University, Siheung-Si, Gyeonggi-do 15073, South Korea

[a)] Contributions: S. T. Yoo and B. C. So contributed equally to this work.
[b)] Authors to whom correspondence should be addressed: kyupark@khu.ac.kr and ohnam@kpu.ac.kr

ABSTRACT

Large area deep ultraviolet (DUV) light is generated by carbon nanotube (CNT) cold cathode electron beam (C-beam) irradiation on $Al_{0.47}Ga_{0.53}N$/$Al_{0.56}Ga_{0.44}N$ multi quantum wells (MQWs) anode. We developed areal electron beam (EB) with CNT cold cathode emitters. The CNT emitters on silicon wafer were deposited with an area of 188 mm^2, and these were vertically aligned and had conical structures. We optimized the C-beam irradiation conditions to effectively excite AlGaN MQWs. When AlGaN MQWs were excited using an anode voltage of 3 kV and an anode current of 0.8 mA, DUV with a wavelength of 278.7 nm was generated in a large area of 303 mm^2. This DUV area is more than 11 times larger than the light emitting area of conventional EB pumped light sources and UV-LEDs.

Electron beam (EB) pumped deep ultraviolet (DUV) light sources and UV light emitting diodes (UV-LEDs) are emerging as alternative UV lighting technologies of excimer lasers and mercury vapor lamps. UV-LEDs have been extensively studied, but their efficiency is low at sub 280 nm due to DUV absorption and lattice mismatch in AlGaN materials.[1–7] One of the alternative techniques to solve these problems is EB pumped DUV light source. Many research groups are working on EB pumping technology for the DUV generation.[7–12] In 2009, K. Watanabe et al. investigated EB pumping on the hexagonal boron nitride (hBN) powder to obtain DUV emission at a wavelength of 225 nm.[8] Also in 2010, Oto et al. reported EB pumping technique with AlGaN multi quantum wells (MQWs), demonstrating high output power of 100 mW.[9] Since then, AlGaN MQWs have been widely used as fluorescent materials with EB pumping for DUV generation.[10–12] Most studies have been performed using thermal electron emitters as an electron source. The conventional technology, in which uses thermal electron source for EB excitation, requires warm-up time to heat a tungsten filament to emit electrons. In the thermal electron sources, the total

power efficiency of the device is significantly low due to power consumption during the warm-up time. The electrons are emitted in all directions, 360 degrees throughout the thermal electron source. However, almost all applications require the electrons to be in the surface normal direction of the anode, since electrons of other directions not utilized. Also, it is very difficult to make flat areal EB for large area DUV lighting. On the other hand, since cold cathode does not require warm-up time and it is easy to make large area electron emitters, cold cathodes can be used as various devices of higher efficiency than thermal electron sources.

Carbon nanotube (CNT) emitters have excellent properties and many groups are researching CNT emitters for vacuum nanoelectronics applications.[13–16] Previously, we used CNT emitters as a cold cathode to generate DUV light with homemade Zn_2SiO_4 anode.[16] CNT emitters were grown on silicon substrate with direct current plasma enhanced chemical vapor deposition (DC-PECVD).[17] Enhanced electron emission properties are attributed to the vertically aligned structure of CNTs which is due to the growth by DC-PECVD and these CNTs are suitable for electron sources

of DUV lighting.[16] As a large area EB irradiation technology, we introduce carbon nanotube cold cathode electron beam (C-beam) pumping technique.

The DUV generation with EB pumping technology has limitations in lighting area, as of today the DUV light emission area is limited to less than 30 mm^2.[8,12] C-beam pumping technology can produce a flat areal UV lamp having a large light emitting area. In the previous work, we fabricated a visible lamp with light emitting area of 25.4 cm^2 using C-beam irradiation on anode phosphor.[18] The light emitting areas depend on the structure of C-beam and the area of the CNT emitters. In this letter, we report the fabrication of large area DUV light with Al$_{0.47}$Ga$_{0.53}$N/Al$_{0.56}$Ga$_{0.44}$N MQWs and the C-beam irradiation pumping technique.

DUV light with Al$_{0.47}$Ga$_{0.53}$N/Al$_{0.56}$Ga$_{0.44}$N MQWs are generated with C-beam of triode structure. Fig. 1 shows schematic of UV lighting system with C-beam pumping. The triode structure of C-beam irradiation is composed of cathode, gate, and anode as shown in Fig. 1(a). C-beam consists of a cathode as an electron source and a gate for electron extraction. As a cold cathode, the vertically aligned high aspect ratio CNT structures are needed for high field enhancement and low threshold voltage for electron emission. The fabricated CNT emitters are shown in the Fig. 1(b), with a height of 40 μm, a tip apex diameter of 60 nm and a CNT bottom contact diameter of 3 μm. CNT emitters are grown on Si wafer by an area of 188 mm^2 and are separated by 30 μm distance to reduce the field screening effect. The gate electrode was used to extract the electrons from the CNT emitters. The distance between the gate and the CNT emitters

was kept at 250 μm by using ceramic insulator. The electron emission characteristics of C-beam is shown in the Fig. 1(c). The cathode current is the current of electrons emitted by the CNT emitters, a key element of the C-beam, and the anode current is the amount of electrons reaching the anode after passing through gate electrode. The gate current is the amount of electrons absorbed in the gate which is also called as the gate leakage current. At the same cathode current, low gate current and high electron transmission rate would result in higher anode current. Also, the power efficiency of the DUV light would be enhanced. In this study, we applied 5 kV at the anode and 1.05 kV at the gate then we obtained the anode current of 1.53 mA. Under this driving condition, we obtained an electron transmission rate of 88.5%, which 11.5% is the cathode current leak through the gate electrode.

The AlGaN MQWs anode was fabricated on c-plane sapphire substrate through high-temperature metal-organic chemical vapor deposition (HT-MOCVD) system. First, the low temperature AlN buffer layer with 25 nm was grown on on-axis sapphire substrate. Then, the 2.2 μm AlN main layer was grown on the AlN buffer layer. AlGaN/AlN superlattice layers (SLs) and n-AlGaN layer were inserted to control the crack and the dislocations associated at the interface between AlN layer and the active region. Finally, the active region consisted of five period Al$_{0.47}$Ga$_{0.53}$N/Al$_{0.56}$Ga$_{0.44}$N was grown on n-AlGaN layer. The detailed growth conditions are described in Refs. 5 and 19.

The shapes of CNT emitters were analyzed using a scanning electron microscope (SEM, Hitachi S-4700). The thin film
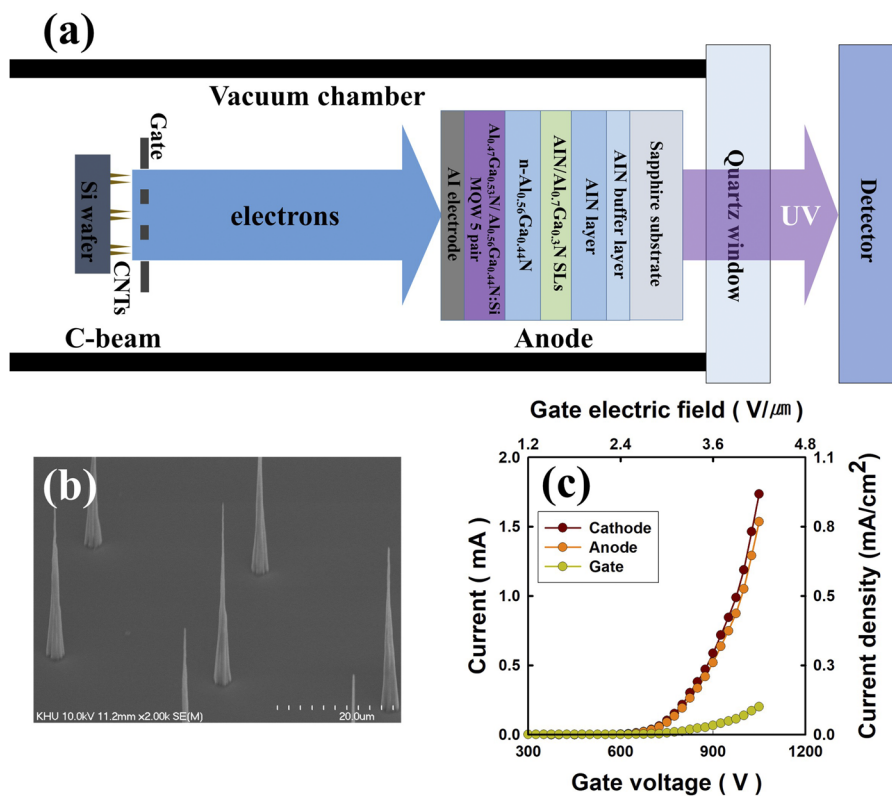

FIG. 1. DUV generation with a carbon nanotube cold cathode based electron beam (C-beam) irradiation: (a) a schematic diagram of deep UV generation; (b) the SEM image of CNT emitters; (c) electron emission characteristics of C-beam.
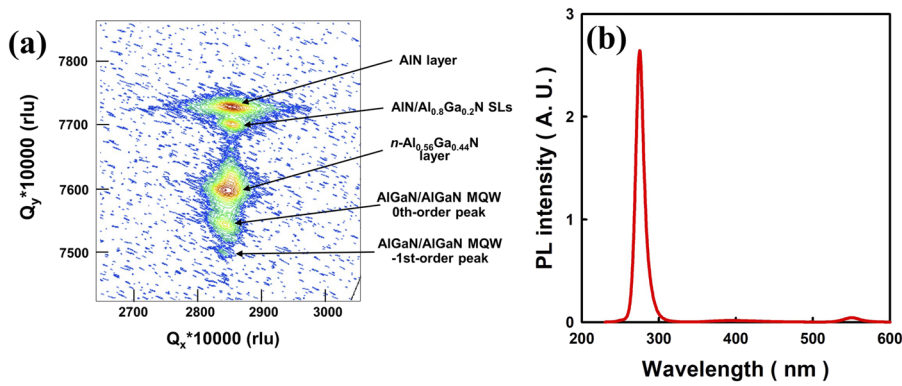
FIG. 2. The properties of $Al_{0.47}Ga_{0.53}N/$ $Al_{0.56}Ga_{0.44}N$ MQWs anode. The results of (a) XRD RSM and (b) PL spectrum of the MQWs.

characteristics of AlGaN MQWs were confirmed by reciprocal space mapping (RSM) measurement using high-resolution X-ray diffraction (HR-XRD, Panalytical X'Pert Pro) and photoluminescence (PL) measurement using a 213nm pulsed laser (CrysLaS Laser Systems, Q-Series). Avaspec-ULS2048 UV spectrometer (Avantes) was used to identify DUV light generated by C-beam pumping. We used Agilent 34401A, Keithley 248 and Spellman SL1200 systems for power supply and current measurements.

Fig. 2(a) shows the XRD RSM around (105) reflection of $Al_{0.47}Ga_{0.53}N/Al_{0.56}Ga_{0.44}N$ MQWs anode. The XRD peaks of the AlN layer, $AlN/Al_{0.8}Ga_{0.2}N$ SLs, AlGaN layer, and $Al_{0.47}Ga_{0.53}N/Al_{0.56}Ga_{0.44}N$ MQWs are clearly observed, respectively. The variation of Q_y related to the different Al composition of epilayers. The Q_x value indicates the stress degree of epilayers. All samples have nearly same Q_x value, which means that the active region consisting of $Al_{0.47}Ga_{0.53}N/Al_{0.56}Ga_{0.44}N$ MQWs are nearly fully strained.[20] PL analysis was performed to investigate the DUV luminescence properties of the prepared AlGaN MQWs anode. When the AlGaN MQWs anode is excited with a wavelength of 213 nm, the PL spectra have a peak wavelength of 275 nm and a FWHM of 12.3 nm as shown in the Fig. 2(b). H. S. Kim et al. reported that the bandgap energy of $Al_xGa_{1-x}N$ varies according to Al content (x) as in (1).[21]

$$Eg(x) = (1 - x)Eg(GaN) + xEg(AlN) - bx(1 - x) \qquad (1)$$

The bandgap energies of GaN and AlN are 3.42 and 6.20 eV at room temperature respectively, and the bowing parameter is

$b = 0.98$ eV. Calculated by substituting x = 0.47 used in MQWs in Equation (1), theoretically, the band gap energy of MQWs is 4.48 eV. It could be confirmed that the MQWs is fabricated as designed with a value similar to the band gap energy of the peak wavelength obtained by the PL measurement, 4.51 eV.

To efficiently excite AlGaN MQWs when using the C-beam pumping technology, proper penetration depth should be studied with variable anode voltage (V_A). Numerous researchers have obtained appropriate penetration depths with various V_A through simulations and experiments.[8–12] The penetration depth with V_A values depend on the electron beam source and anode structure, but V_A below 10 kV is required when the thickness of active layer is less than 100 nm.[10,11] In order to perform C-beam pumping on the $Al_{0.47}Ga_{0.53}N/Al_{0.56}Ga_{0.44}N$ MQWs anode, the penetration depth of electrons according to V_A was investigated. Fig. 3 shows UV luminescence characteristics with various V_A. The anode current (I_A) is fixed at 0.2 mA to reduce anode heating. Fig. 3(a) shows the UV spectra with various V_A. When V_A is 3 kV, a single peak with a wavelength of 278.7 nm is observed. As the V_A increased, the UV intensity was slightly enhanced with the increased input power. When V_A increases more than 4 kV, new emission peak is observed near the wavelength of 320 nm. Fig. 3(b) shows the peak wavelength and the irradiance with various V_A. The peak wavelength increases with V_A up-to 5kV, after which becomes saturated. This is because of the change in peak wavelength due to an increase in peak intensity at a wavelength of about 320 nm, not due to a change in peak at a wavelength of 278.7 nm.
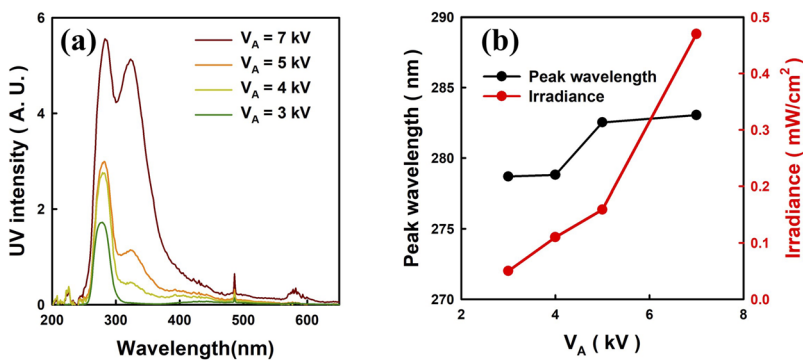

FIG. 3. Characteristics of UV luminescence with anode bias. I_A fixed at 0.2 mA. (a) UV spectra with various anode bias. (b) Peak wavelength and irradiance change with variable anode bias.
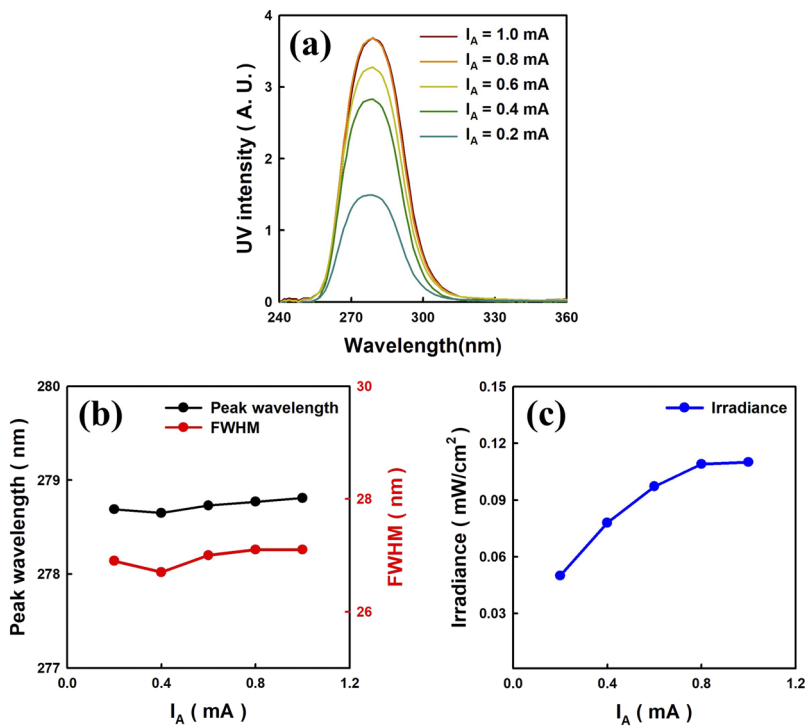
FIG. 4. Characteristics of UV luminescence with anode current. V_A fixed at 3 kV. (a) UV spectra with variable anode current. (b) The variation of peak wavelength and FWHM with anode current. (c) Irradiance with anode current.

We fixed the V_A at 3 kV to produce a single peak DUV light similar with the PL spectra in Fig. 2(b). Fig. 4 shows the characteristics of UV emission with various I_A. Fig. 4(a) shows that a single peak with a wavelength of 278.7 nm occurs regardless of the change in I_A. The peak wavelength and FWHM with I_A are shown in Fig. 4(b), and the irradiance variation are shown in Fig. 4(c). Even change in I_A, the peak wavelength and FWHM is maintained at about 278.7 nm and 27 nm, respectively. However, the irradiance as shown in Fig. 4(c) increases with I_A. When I_A is greater than 0.8 mA, the irradiance is saturated to 0.11 mW/cm^2. When compared to Fig. 3, the peak at the wavelength near 320 nm was not detected in Fig. 4 at V_A of 3 kV with I_A up to 1.0 mA. In Fig. 3, we found 320 nm UV peak at the V_A of 4 kV and I_A of 0.2 mA. In this driving condition, the power delivered on the anode is 0.8 watt. However, in the case of V_A of 3 kV, we could not find 320 nm UV peak up-to anode power of 3 watt. From this comparison, the origin of the 320 nm peak is not due to heat effect of the power but the UV peak near the 320 nm wavelength had appeared from defect states in MQWs.

Based on these studies, we tried to make flat areal DUV light with a large light emitting area. Fig. 5 shows the light emission image generated by C-beam pumping on AlGaN MQWs. In order to generate a single peak with a wavelength of 278.7 nm, the C-beam irradiation condition was maintained at 3 kV of V_A and 0.8 mA of I_A. As can be easily seen from the eye, we found visible light of blue color and the emission area is well-overlapped with UV emission area as confirmed by a UV spectrometer. The blue light comes from cathodoluminescence by the excitation of defect states in MQWs with C-beam irradiation. The UV light emission area of 303 mm^2 was obtained by image analysis using the image J program, as shown in Fig. 5(b). The UV lighting area is 1.6 times larger than CNT

emitter area of 188mm^2. S. I. Inoue et al. fabricated DUV-LEDs with mesa size of 0.35 mm^2.[6] In the case of EB pumping, K. Watanabe et al. obtained the highest emission area of 27.2 mm^2 using EB pumping on the hBN powder.[8] The DUV light emitting area of ~303 mm^2 we obtained using C-beam pumping is 11 times larger than the previous studies.

In conclusion, large area DUV light was successfully obtained by using C-beam irradiation pumping technique on the $Al_{0.47}Ga_{0.53}N/Al_{0.56}Ga_{0.44}N$ MQWs anode. We fabricated 188 mm^2 CNT emitters on Si wafers to obtain large area DUV light. The C-beam shows high electron transmittance through the gate electrode of 88.5%. $Al_{0.47}Ga_{0.53}N/Al_{0.56}Ga_{0.44}N$ MQWs, which were
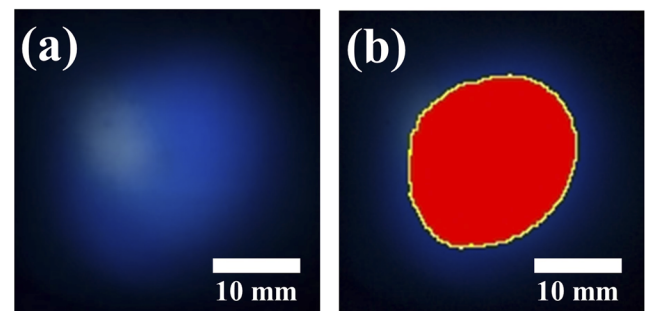

FIG. 5. Light emission image generated by C-beam pumping on AlGaN MQWs. The C-beam irradiation condition was kV for V_A and 0.8 mA for I_A. (a) The optical image of 278.7 nm deep UV lighting. The red area of (b) represent light emitting area analyzed in image J. The light emitting area is 303 mm^2.

prepared by HT-MOCVD on c-plane sapphire substrate. With optimization of anode bias and current, we obtained a large area DUV light of 303 mm^2 with a wavelength of 278.7 nm. At this time, C-beam was irradiated at the V_A of 3 kV and I_A of 0.8 mA. Large-area DUV light sources using C-beam pumping open up the potential of UV devices used in a variety of fields such as disinfection, deodorization, photo catalysis, and gas detection.

REFERENCES

[1] J. Chen, S. Loeb, and J.-H. Kim, Environ. Sci.: Water Res. **3**, 188 (2017).

[2] H. Hirayama, N. Maeda, S. Fujikawa, S. Toyoda, and N. Kamata, Jpn. J. Appl. Phys. **53**, 100209 (2014).

[3] N. Maeda and H. Hirayama, Phys. Status Solidi (C) **10**, 1521 (2013).

[4] T. Takano, T. Mino, J. Sakai, N. Noguchi, K. Tsubaki, and H. Hirayama, Appl. Phys. Express **10**, 031002 (2017).

[5] B. So, J. Kim, E. Shin, T. Kwak, T. Kim, and O. Nam, Phys. Status Solidi (A) **215**, 1700677 (2017).

[6] S. Inoue, N. Tamari, and M. Taniguchi, Appl. Phys. Lett. **110**, 141106 (2017).

[7] D. Li, K. Jiang, X. Sun, and C. Guo, Adv. Opt. Photon. **10**, 43 (2018).

[8] K. Watanabe, T. Taniguchi, T. Niiyama, K. Miya, and M. Taniguchi, Nat. Photonics **3**, 591 (2009).

[9] T. Oto, R. G. Banal, K. Kataoka, M. Funato, and Y. Kawakami, Nat. Photonics **4**, 767 (2010).

[10] T. Matsumoto, S. Iwayama, T. Saito, Y. Kawakami, F. Kubo, and H. Amano, Opt. Express **20**, 24320 (2012).

[11] H. Sun, J. Woodward, J. Yin, A. Moldawer, E. F. Pecora, A. Y. Nikiforov, L. Dal Negro, R. Paiella, K. Ludwig, Jr., D. J. Smith, and T. D. Moustakas, J. Vac. Sci. Technol. B **31**, 03C117 (2013).

[12] F. Tabataba-Vakili, T. Wunderer, M. Kneissl, Z. Yang, M. Teepe, M. Batres, M. Feneberg, B. Vancil, and N. M. Johnson, Appl. Phys. Lett. **109**, 181105 (2016).

[13] M. F. L. De Volder, S. H. Tawfick, R. H. Baughman, and A. J. Hart, Science **339**, 535 (2013).

[14] Y. C. Choi, J.-T. Kang, S. Park, M.-S. Shin, H. Jeon, J.-W. Kim, J.-W. Jeong, and Y.-H. Song, Carbon **100**, 302 (2016).

[15] H. R. Lee, H. H. Yang, and K. C. Park, J. Vac. Sci. Technol. B **35**, 06G804 (2017).

[16] S. T. Yoo, J. H. Hong, J. S. Kang, and K. C. Park, J. Vac. Sci. Technol. B **36**, 02C103 (2018).

[17] S. H. Lim, K. C. Park, J. H. Moon, H. S. Yoon, D. Pribat, Y. Bonnassieux, and J. Jang, Thin Solid Films **515**, 1380 (2006).

[18] S. T. Yoo, J. S. Kang, and K. C. Park, J. Nanosci. Nanotechnol. **17**, 7362 (2017).

[19] B. So, J. Kim, T. Kwak, T. Kim, J. Lee, U. Choi, and O. Nam, RSC Adv. **8**, 35528 (2018).

[20] S. Fan, Z. Qin, C. He, X. Wang, B. Shen, and G. Zhang, Opt. Express **22**, 6322 (2014).

[21] H. S. Kim, R. A. Mair, J. Li, J. Y. Lin, and H. X. Jiang, Appl. Phys. Lett. **76**, 1252 (2000).